



Intestinal Pathology and Gut Microbiota Alterations in a Methyl-4-phenyl-1,2,3,6-tetrahydropyridine (MPTP) Mouse Model of Parkinson's Disease

Feng Lai¹ · Rong Jiang² · Wenjun Xie¹ · Xinrong Liu¹ · Yong Tang³ · Hong Xiao¹ · Jieying Gao¹ · Yan Jia¹ · Qunhua Bai¹

Received: 6 June 2018 / Revised: 3 August 2018 / Accepted: 21 August 2018 / Published online: 31 August 2018
© Springer Science+Business Media, LLC, part of Springer Nature 2018

Abstract

Patients with Parkinson's disease (PD) often have non-motor symptoms related to gastrointestinal (GI) dysfunction, such as constipation and delayed gastric emptying, which manifest prior to the motor symptoms of PD. Increasing evidence indicates that changes in the composition of the gut microbiota may be related to the pathogenesis of PD. However, it is unclear how GI dysfunction occurs and how gut microbial dysbiosis is caused. We investigated whether a neurotoxin model of PD induced by chronic low doses of MPTP is capable of reproducing the clinical intestinal pathology of PD, as well as whether gut microbial dysbiosis accompanies this pathology. C57BL/6 male mice were administered 18 mg/kg MPTP twice per week for 5 weeks via intraperitoneal injection. GI function was assessed by measuring the 1-h stool frequency and fecal water content; motor function was assessed by pole tests; and tyrosine hydroxylase and alpha-synuclein expression were analyzed. Furthermore, the inflammation, intestinal barrier and composition of the gut microbiota were measured. We found that MPTP caused GI dysfunction and intestinal pathology prior to motor dysfunction. The composition of the gut microbiota was changed; in particular, the change in the abundance of *Lachnospiraceae*, *Erysipelotrichaceae*, *Prevotellaceae*, *Clostridiales*, *Erysipelotrichales* and *Proteobacteria* was significant. These results indicate that a chronic low-dose MPTP model can be used to evaluate the progression of intestinal pathology and gut microbiota dysbiosis in the early stage of PD, which may provide new insights into the pathogenesis of PD.

Keywords Parkinson's disease · MPTP · Intestinal pathology · Gut microbiota

Introduction

Parkinson's disease (PD) is a progressive neurological disorder characterized by tremor, rigidity, bradykinesia and postural instability [1]. The pathological features of PD include

the appearance of Lewy bodies, which are mainly composed of alpha-synuclein (α -syn), and the death of dopaminergic (DAergic) neurons in the substantia nigra pars compacta (SNpc) [2]. In addition to movement disorder, patients present non-motor symptoms, including depression, cognitive impairment, sleep disorders, hyposmia and, most generally, gastrointestinal (GI) dysfunction [2, 3]. Patients have constipation, delayed gastric emptying, defecation problems and other GI dysfunction, which can all affect their quality of life [4]. Recently, researchers have reported that PD patients have gastrointestinal tract (GIT) pathology, such as increased intestinal permeability [5] and gut microbial dysbiosis [6], which may play an important role in the course of PD.

The GIT is an important portal for external pathogenic factors, such as poisons and pathogens, to enter the body. The current theory that explains the pathogenesis of PD from the gut to the brain is Braak staging [7]. The study introducing this theory demonstrated that α -syn appears in the enteric nervous system (ENS) during the early stages

Electronic supplementary material The online version of this article (<https://doi.org/10.1007/s11064-018-2620-x>) contains supplementary material, which is available to authorized users.

✉ Qunhua Bai
1253811562@qq.com

- ¹ School of Public Health and Management, Chongqing Medical University, 1 Yi Xue Yuan Road, Chongqing 400016, People's Republic of China
- ² School of Basic Medicine, Chongqing Medical University, Chongqing 400016, People's Republic of China
- ³ Chongqing Orthopedics Hospital of Traditional Chinese Medicine, Chongqing 400016, People's Republic of China

of PD, and this misfolded protein may spread to the central nervous system (CNS) through the vagus nerve, resulting in nerve damage in the substantia nigra (SN) [8, 9]. Animal model studies have indicated that intraperitoneal administration of toxicants may cause damage and pathology in the GI nerves [10–12]. Therefore, GI nerves may be quite sensitive to internal and external injury factors. However, how the damage of GI nerves occurs in PD is not entirely clear.

The gut microbiota can participate in the regulation of the brain–gut axis function by affecting nervous, endocrine, and immune signaling mechanisms, thereby influencing neurologic pathologies, such as anxiety, depression, autism spectrum disorder and Alzheimer's disease [13–16]. Interestingly, increasing evidence indicates that alterations in the composition of the gut microbiota and microbial metabolites may be related to the pathogenesis and clinical phenotype of PD [17]. The intestinal environment is an important environmental factor that affects the gut microbiota. Therefore, GI dysfunction, an abnormal intestinal state that occurs in PD, may disturb the gut microbiota, and they may also influence each other. However, it is unclear how GI dysfunction occurs and what role it plays in PD.

Inflammation influences the pathogenesis and progression of PD [12]. Proinflammatory cytokines and activation of microglia lead to persistent chronic inflammation during neurodegeneration [18, 19]. Microglia are important immune cells in the brain, and ionized calcium-binding adaptor molecule-1 (Iba1), a marker constitutively expressed by microglia, is upregulated as a result of microglial activation [20, 21].

Animal models contribute to understanding the pathological damage involved in PD. Methyl-4-phenyl-1,2,3,6-tetrahydropyridine (MPTP), 6-hydroxydopamine (6-OHDA) and rotenone are common poisons used to build PD models [22]. MPTP, a neurotoxin, is metabolized to the toxin 1-methyl-4-phenylpyridine (MPP⁺) by monoamine oxidase B (MAO-B) and is taken up by DAergic neurons, where it eventually leads to neuronal death [23, 24]. MPTP can produce DAergic selective neuron toxins in the ENS of animal models, causing damage to neurons [10, 11, 25]. This is a good model for observing PD-related GI dysfunction. In this model, it is clear that the damage of DAergic neurons is an initial factor.

In this study, we constructed a PD animal model using chronic low doses of MPTP. At two time points (2 days and 3 weeks after the last MPTP administration), we evaluated (1) the presence of SN lesions, whether MPTP-induced neuronal damage in the intestine caused intestinal pathological changes and (2) whether gut microbial dysbiosis accompanied this pathology at different time points. These results will help elucidate the intestinal pathogenesis and composition of the gut microbiota in PD.

Materials and Methods

Animals

C57BL/6 male mice, specific-pathogen-free (SPF) grade, were purchased from Chongqing Medical University Laboratory Animal Center (Chongqing, China). Mice were housed (5 mice/cage, 12 h light/dark cycle) under pathogen-free conditions in a mean constant temperature (25 ± 1.0 °C) with 60–70% relative humidity and had access to food and water ad libitum. The ethics committees of Chongqing Medical University approved all animal experiments.

MPTP Treatments

Mice were divided into control and MPTP groups (20 per group). The MPTP group was treated with MPTP (18 mg/kg i.p.; Sigma-Aldrich, St. Louis, MO, USA) twice a week in the afternoon (Tuesday and Saturday) for 5 weeks, whereas the control group was injected with a standard suspension vehicle (0.9% NaCl, w/v). The mice were weighed at each injection and once per week after administration.

Motor and GI Function

Behavior and GI function were evaluated at different time points after MPTP administration (2 days after the fifth administration and 2 days and 3 weeks after the last injection, $n = 10:5$ control/5 MPTP).

In the pole test, a cork ball (2.5 cm diameter) was fastened to the top of a standing pole (1 cm diameter and 50 cm length) that was wrapped with gauze to avoid slipping. After the mouse was put on the cork ball, the time needed for the mouse to climb the upper and lower halves of the pole was recorded. The judging standards were as follows: a score of three for time ≤ 3 s, a score of two for $3 < \text{time} \leq 6$ s and a score of one for time > 6 s. The results were shown as the sum of the scores [26].

In the GI function tests, the animals were fasted overnight. The next day, the mice were given access to food for 2 h prior to testing. The animals were placed in clean isolated metabolic cages for 1 h. Feces were collected, counted and weighed, and subsequently dried overnight at 65 °C to assess the fecal dry weight [27]. The research design is summarized in Fig. 1.

Sample Collection

Two days ($n = 20:10$ control/10 MPTP) or 3 weeks ($n = 20:10$ control/10 MPTP) after the final MPTP

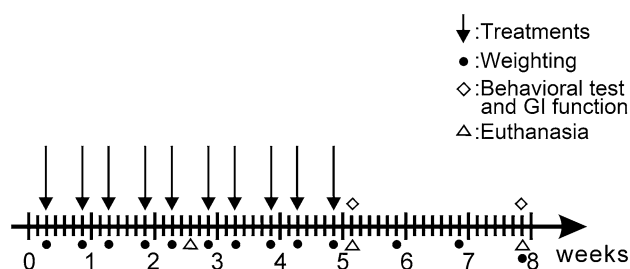


Fig. 1 Timeline of treatments, weighing, behavioral experiments, GI function tests and euthanasia. Mice were treated twice per week (Tuesday and Saturday) for 5 weeks. Mice were weighed at each injection and once per week after administration. Behavioral and GI function tests were performed at 2 days after the fifth administration and 2 days and 3 weeks after the last injection. The mice were sacrificed at 2 days or 3 weeks after the last injection. *GI* gastrointestinal

administration, the animals were anesthetized via excess pentobarbital sodium (Lethobarb, Virbac, Australia).

We collected blood from the retro-orbital sinus and fresh SN, striatum and segments of the ileum by dissection. The blood samples were stored overnight at 4 °C, and after 3000 r/min (4 °C, 10 min) centrifugation, the supernatant was stored at –20 °C for enzyme-linked immunosorbent assay (ELISA). Tissues (SN, striatum and segments of the ileum) for western blot (WB) analysis, dopamine (DA) content determination and ELISA were frozen in liquid nitrogen and stored at –80 °C. Ileum samples were prepared as wholemounts as subsequently described.

For immunohistochemistry (IHC) of the ileum and immunofluorescence (IF) of the SN, after anesthesia, the mice received a transcardial perfusion of saline followed by 4% paraformaldehyde (pH 7.4). Segments of the ileum were fixed with 4% paraformaldehyde overnight and embedded in paraffin. The brain samples were maintained in 20% sucrose for 24 h and then in 30% sucrose for 24 h; the samples were then stored at –80 °C.

Wholemount Preparation

To inhibit the contraction of ileal tissue, we placed the tissue in phosphate-buffered saline (PBS) that contained the L-type calcium channel blocker nifedipine (10^{-6} M; Sigma, Castle Hill, Sydney, Australia). The contents of the ileum were purged with PBS. Several segments of the ileum were prepared as wholemounts as previously reported [28]. Briefly, the segments of the ileum were pinned to balsa wood sheets for fixation in 2% formaldehyde plus 0.2% picric acid in 0.1 M PBS, at 4 °C overnight. The fixative was cleared by washing in dimethyl sulfoxide followed by PBS. The fixed tissue was stored at 4 °C in PBS that contained sodium azide (0.1%) for IF. Myenteric plexus (MP) preparations were obtained by removing the mucosa.

ELISA

The concentrations of interleukin-17 (IL-17), interleukin-1 β (IL-1 β), and tumor necrosis factor- α (TNF- α) in the SN and ileum were detected using commercial ELISA kits (Boster Biotech, Wuhan, China). D-Lactic acid (D-LAC) and diamine oxidase (DAO) levels in the serum were measured using a D-LAC ELISA kit (Jingkang, Shanghai, China) and a DAO ELISA kit (Cusabio Biotech, Wuhan, China), respectively. All experiments were implemented according to the manufacturer's instructions.

DA Analysis by Liquid Chromatography–Mass Spectrometry (LC–MS)

Samples of ileum and striatum were added to an appropriate amount of extract [water:methanol (1:3, v/v)] and mixed with the internal standard application solution (Sigma-Aldrich, St. Louis, MO, USA). After homogenization, the supernatant was collected by refrigerated centrifugation at 15,000 rpm for 15 min, and then concentrated in vacuo to dry after derivatization. The derivatization reaction proceeded as follows: moderate sodium bicarbonate (pH=11.0, 0.2 M) solution and dansyl chloride (2 mg/mL) solution were added to the evaporated sample, vortexed for 1 min, and subsequently reacted in 60 °C water. The reaction solution was centrifuged at 18,000 rpm for 10 min, and 5 μ L of the collected supernatant were injected into the column.

The quantitation of DA in the ileum and striatum was performed on a Thermo Scientific Dionex Ultimate 3000 RSLC system fitted with a Thermo Hypersill GOLD column (2.1 \times 100 mm, 1.7 μ m) and a Thermo Q Exactive Orbitrap mass spectrometer equipped with a heated electrospray ionization source (HESI-II) with a positive ionization mode and nitrogen as the collision gas and damping gas. The selected ions for DA were 427.12 *m/z*. Instrument control and analyses were performed with Thermo Xcalibur 2.2 software.

Western Blot

Protein extraction was performed by homogenizing a suitable amount of tissue in radioimmunoprecipitation assay (RIPA) buffer (Beyotime, Shanghai, China) with phenylmethylsulphonyl fluoride (PMSF, 1 mM) (Beyotime, Shanghai, China). After centrifugation at 12,000 rpm, 4 °C for 10 min, the protein content in the supernatant was quantified using a bicinchoninic acid (BCA) Protein Assay Kit (Beyotime, Shanghai, China). After the supernatant was denatured with sodium dodecyl sulfate-polyacrylamide gel electrophoresis (SDS-PAGE) Sample Loading Buffer (Beyotime, Shanghai, China), the proteins were separated by SDS-PAGE and transferred to polyvinylidene fluoride (PVDF) membranes. The membranes were subsequently incubated

with antibodies (Table 1) overnight at 4 °C. Goat anti-rabbit IgG (1:4000, Boster Biotech, Wuhan, China) was used as the secondary antibody. Anti-beta-actin antibody (Table 1) was used as an internal control. All bands were detected with an enhanced chemiluminescence kit (Millipore, Billerica, MA, USA) and imaged using a Gel Image System (BioRad, CA, USA). The density was measured using Quantity One® software.

Immunohistochemistry

Briefly, slices were placed in citric acid buffer (0.01 M) and heated in a microwave for 20 min to repair the antigens. After microwave reparation, sample preparation was performed according to the kit instructions (Zhongshan Biotech, Beijing, China). The sections were then colored with Diaminobenzidine (DAB, Zhongshan Biotech, Beijing, China), stained again, dehydrated using an ethanol gradient, transparentized with dimethylbenzene, and mounted with neutral gum. Images were obtained using a microscope.

Immunofluorescence

Mouse brains were cut into 35 µm slices with a frozen sliding microtome, and the SN fractions were also collected. After blocking in phosphate-buffered saline with Triton-X-100 [PBST, 2% (w/v) bovine serum albumin (BSA), 0.3% Triton-X-100, 0.01 M PBS], slices or wholemounts were incubated at 4 °C for 48 h with antibodies (TH, Iba1, α-syn) (Table 1). Goat anti-rabbit immunoglobulin G (IgG, 1:75, BA1105, Boster Biotech, Wuhan, China) conjugated to fluorescein isothiocyanate (FITC) was used as a secondary antibody. Images were obtained using a microscope.

Fecal Microbiota Profiling

Total Microbial DNA was extracted from fecal samples with the E.Z.N.A.® Soil DNA kit (Omega Biotek, Norcross, GA, USA) The V3–V4 regions of the bacterial 16S rRNA gene were used as the bacteria-specific fragment and were amplified with primers 338F (5'-ACTCCTACGGGA

GGCAGCAG-3') and 806R (5'-GGACTACHVGGGTWTCTAAT-3') using a thermocycler polymerase chain reaction (PCR) system (GeneAmp 9700, ABI, USA). The purified amplicons were quantified and sequenced on an Illumina MiSeq platform (Illumina, San Diego, USA) with paired-end sequencing (2 × 300). The raw sequences were analyzed using QIIME and UPARSE as previously described [29] and were binned into operational taxonomic units (OTUs) at 97% identity and matched to entries in the SILVA128 at a 70% confidence level. The bacterial α-diversity was calculated by the biodiversity index (ACE, Chao, Sobs, Shannon, and Simpson). β-Diversity was measured using the Bray–Curtis distance and displayed using hierarchical clustering and principal component analysis (PCA). In addition, we analyzed the differences in the microbial composition and relative abundance of each group.

Statistical Analysis

Statistical analysis was performed using one-way analysis of variance (ANOVA) with Bonferroni post-tests for normally distributed and variance homogenized data and nonparametric tests for other data with SPSS 22.0 software (IBM Corporation, Armonk, NY, USA). The results are presented as the mean ± standard deviation, and $P < 0.05$ was considered statistically significant (* $P < 0.05$, ** $P < 0.01$, *** $P < 0.001$). All data are presented using GraphPad Prism version 7.0 statistical software (GraphPad, Inc., La Jolla, USA).

Results

MPTP Influences the General Condition of Mice

Following the administration of MPTP, general conditions, such as the motor ability, body weight, and defecation status of mice, have been reported to change, indicating that the animals respond to MPTP administration. Weight and behavioral tests were not significantly affected (data not shown). To determine whether GI dysfunction exists under MPTP treatment, the 1-h stool frequency and fecal water content

Table 1 Primary antibodies used for western blot, immunohistochemistry and immunofluorescence

Tissue antigen	Host species	Dilution			Reference ^a
		WB	IHC	IF	
Tyrosine hydroxylase (TH)	Rabbit	1:200	–	1:1000	Abcam ab112
Inducible nitric oxide synthase (iNOS)	Rabbit	1:200	1:100	–	Abcam ab15323
α-Synuclein	Rabbit	1:1000	–	1:200	CST D37A6
Ionized calcium binding adaptor molecule 1 (Iba1)	Rabbit	1:1000	–	1:100	Abcam ab178847
Beta-actin	Rabbit	1:2500	–	–	Bioss bs-0061R

^aSuppliers: Abcam plc, Cambridge, United Kingdom; Cell Signaling Technology, Beverly, MA, USA; Bioss, Beijing, China

were measured (Fig. 2). At 16, 34 and 53 days after the first MPTP administration, the 1-h stool frequency of MPTP-treated mice was significantly lower than that of control mice (Fig. 2a). Moreover, after the first MPTP administration, the stool frequency decreased at the 34th day compared with that at the 16th day and substantially recovered at the 53rd day (Fig. 2a). The fecal water content of MPTP-treated mice at the 34th day was significantly lower than that of control mice. At the 53rd day, there was no significant difference between the control and the MPTP-treated mice. Additionally, there was an increase at the 53rd day compared with that at the 34th day (Fig. 2b). These results suggest that MPTP induces GI dysfunction in PD mice.

MPTP Reduces the Striatal and Ileal DA Content of Mice

The concentration of DA indicates the ability of DAergic neurons to compound and release DA, and it can simultaneously reflect the degree of damage to DAergic neurons. As measured by LC–MS, the striatal DA levels in MPTP-treated

mice were remarkably decreased by 41.5% and 13.3% compared with those in control mice at 2 days and 3 weeks post-treatment, and the DA levels were higher at the later time point (Fig. 3a). In the ileum, the DA concentration decreased by 49.7% and 16.8% at these two time points compared with the control, and DA was also higher at 3 weeks post-treatment (Fig. 3b). These results suggest that MPTP induced a decrease in the DA concentration in the striatum and ileum.

MPTP Affects TH and α -Syn Expression in the SN of Mice

TH is the rate-limiting enzyme for DA synthesis. To investigate the influence of MPTP on DAergic neurons and TH expression in the SN, WB and IF experiments were used to characterize TH expression. WB analysis of the SN displayed a prominent decrease in TH expression in mice at 2 days and 3 weeks post-treatment compared with the control. Additionally, at 3 weeks post-treatment, the expression was lower than that at 2 days post-treatment (Fig. 4a). IF analysis displayed a significant loss of TH immunoreactivity

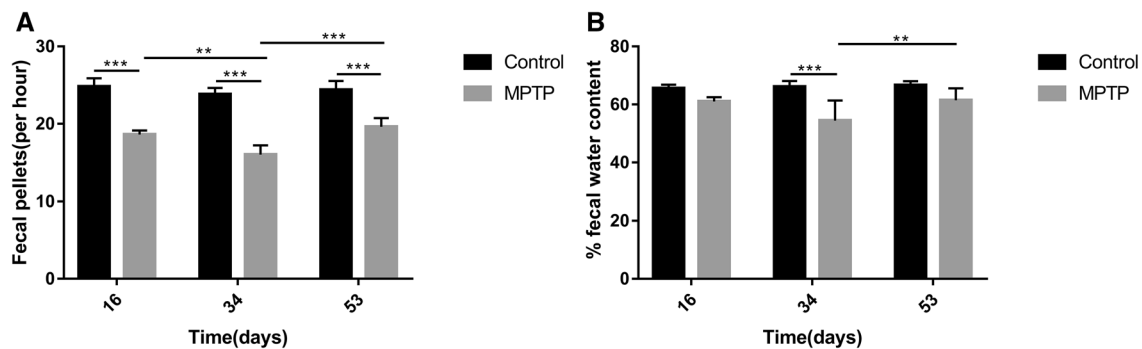


Fig. 2 MPTP induces GI dysfunction. **a** 1-h fecal pellets and **b** percent fecal water content over the course of the study. Feces were collected at 2 days after the fifth administration and 2 days and 3 weeks

after the last injection. * $P < 0.05$, ** $P < 0.01$, *** $P < 0.001$. Error bars are SD ($n = 5$). MPTP methyl-4-phenyl-1,2,3,6-tetrahydropyridine, GI gastrointestinal, SD standard deviation

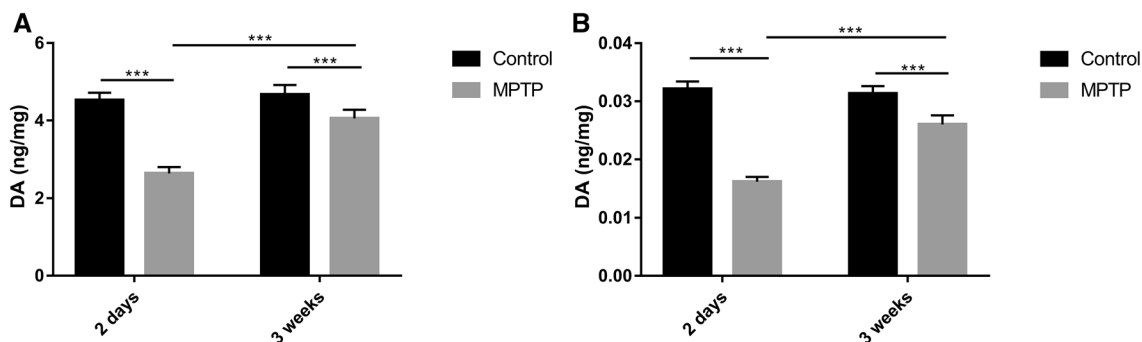
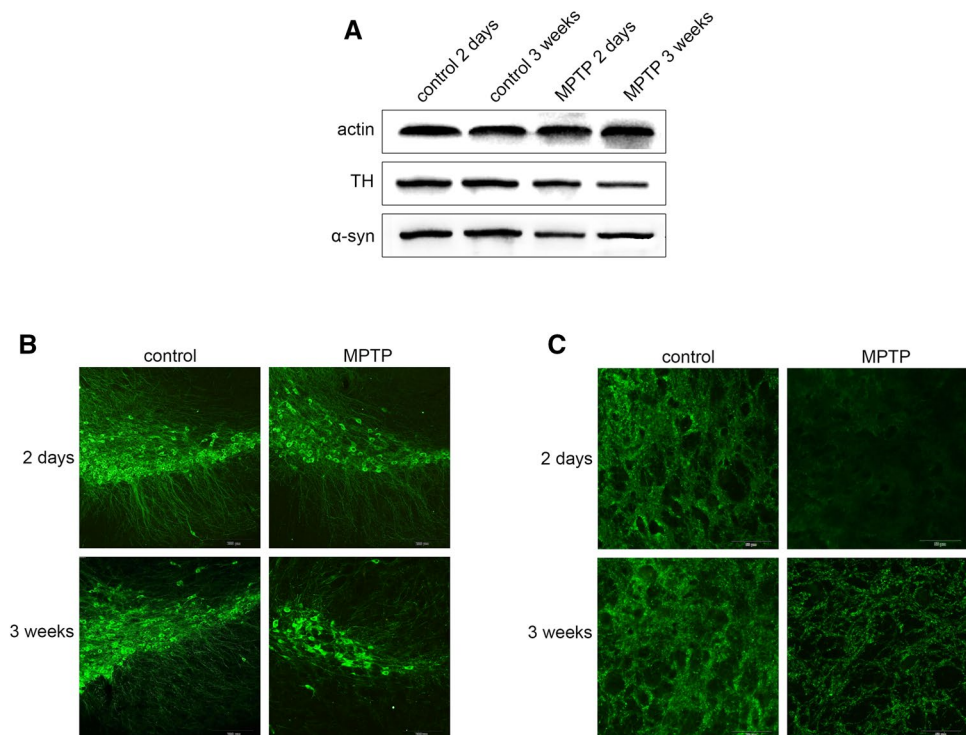


Fig. 3 MPTP reduces the DA content in the striatum (**a**) and ileum (**b**). The DA content was measured by LC–MS at 2 days and 3 weeks after the last injection. *** $P < 0.001$. Error bars are SD ($n = 3$). MPTP

methyl-4-phenyl-1,2,3,6-tetrahydropyridine, DA dopamine, LC–MS liquid chromatography–mass spectrometry, SD standard deviation

Fig. 4 MPTP influences TH and α -syn expression in the SN. **a** Representative WB of nigral TH and α -syn expression. **b** Representative IF staining for TH in the SN. Scale bar is 200 μ m. **c** Representative IF staining for α -syn in the SN. Scale bar is 50 μ m. *MPTP* methyl-4-phenyl-1,2,3,6-tetrahydropyridine, *TH* tyrosine hydroxylase, *α -syn* alpha-synuclein, *SN* substantia nigra, *WB* western blot, *IF* immunofluorescence



in mice at 2 days and 3 weeks, and over time, the trend towards a decrease was more obvious (Fig. 4b).

One of the pathological hallmarks of PD is the presence of Lewy bodies and Lewy neurites formed by the abnormal accumulation of α -syn. To observe whether there is a similar pathology in the SN of MPTP-treated mice, the expression of α -syn was measured. WB analysis of SN showed that α -syn expression in mice at 2 days and 3 weeks post-treatment was lower than in the respective control mice, whereas mice at 3 weeks post-treatment displayed increased expression compared with mice at 2 days post-treatment (Fig. 4a). IF staining in the SN revealed that MPTP produced a remarkable decrease in α -syn of mice at 2 days and 3 weeks post-treatment, and the decrease was greater in mice at 2 days post-treatment (Fig. 4c).

These results indicate that MPTP influences the expression of TH and α -syn in the SN.

MPTP Affects TH and α -Syn Expression in the Ileum of Mice

We also assessed the expression of TH and α -syn in the ileum. Two days and 3 weeks after the treatment ended, WB analysis of TH expression showed an increase compared to the respective control, and the increasing trend was more apparent in mice at 2 days post-treatment than at 3 weeks post-treatment (Fig. 5a). IF analysis indicated that MPTP produced a prominent increase in TH expression in the ileum of mice at 2 days post-treatment. However, compared with

control mice, mice at 3 weeks post-treatment showed a slight increase (Fig. 5b).

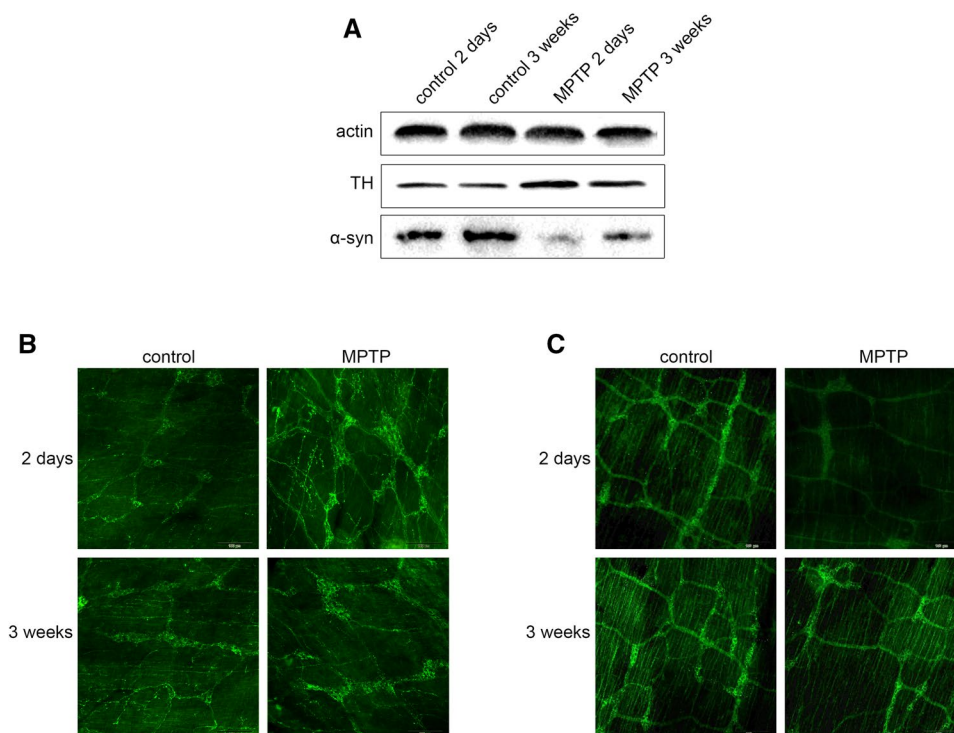
Consistent with the results for the SN, WB and IF analyses of α -syn expression in the ileum indicated that there was a decrease at the two time points compared with the respective control, and α -syn was higher at 3 weeks post-treatment than 2 days post-treatment (Fig. 5a, c).

These results indicate that MPTP influences the expression of TH and α -syn in the ileum.

MPTP Causes SN Inflammation in Mice

Inflammation influences the pathogenesis and progression of PD [12]. Microglia are important immune cells in the brain. Activation of microglia leads to persistent chronic inflammation during neurodegeneration [18]. To determine the activation state of the microglia, we measured the expression of Iba1 in the SN using WB and IF. WB results showed that Iba1 expression was higher in mice at 2 days and 3 weeks post-treatment than in control mice, and Iba1 expression showed a higher increase at 2 days post-treatment than at 3 weeks post-treatment (Fig. 6a). IF staining showed that at 2 days and 3 weeks after the last MPTP injection, more microglia were activated in the SN than in the respective control, and there were fewer activated microglia at 3 weeks post-treatment than at 2 days post-treatment (Fig. 6b). To further explore the specific inflammatory state in the SN, we measured the expression levels of IL-17, IL-1 β and TNF- α by ELISA. We observed that the expression levels

Fig. 5 MPTP influences TH and α -syn expression in the ileum. **a** Representative WB of TH and α -syn expression in the MP. **b**, **c** Representative IF staining for TH and α -syn in the MP. Scale bar is 100 μ m. *MPTP* methyl-4-phenyl-1,2,3,6-tetrahydropyridine, *TH* tyrosine hydroxylase, *α -syn* alpha-synuclein, *WB* western blot, *MP* myenteric plexus, *IF* immunofluorescence



of IL-17, IL-1 β and TNF- α were higher by 93.6%, 223.8% and 126.7%, respectively, in the SN of mice at 2 days post-treatment, and higher by 29.4%, 120.4% and 61.6%, respectively, in mice at 3 weeks post-treatment compared with those in the respective control groups. However, the IL-17 results showed an increasing trend, which was not statistically significant, between control mice and mice at 3 weeks post-treatment. At 3 weeks post-treatment, mice displayed levels of IL-17, IL-1 β and TNF- α that were 38.0%, 43.9% and 32.6% lower, respectively, compared with mice at 2 days post-treatment (Fig. 6c–e).

In conclusion, MPTP-treated mice may develop SN inflammation.

MPTP Causes Gut Inflammation in Mice

Inflammation plays a crucial role in the GI degeneration induced by MPTP [30]. To understand the intestinal inflammation present in PD, we characterized the expression of inducible nitric oxide synthase (iNOS) in the ileum by WB and IHC and measured the levels of IL-17, IL-1 β and TNF- α in the ileum by ELISA.

As expected, WB results showed that iNOS expression was increased in mice at 2 days and 3 weeks post-treatment compared with that in the respective control mice, and iNOS expression was higher at 2 days post-treatment than at 3 weeks post-treatment (Fig. 7a). The IHC results also showed that iNOS expression was increased in the ileum in mice at 2 days and 3 weeks post-treatment compared to that

in the respective control mice, and the iNOS levels were decreased in mice at 3 weeks post-treatment compared with those in mice at 2 days post-treatment.

We found that the expression levels of IL-17, IL-1 β and TNF- α in the ileum were 103.6%, 209.4% and 179.0% higher, respectively, in mice at 2 days post-treatment than in control mice and 31.9%, 35.4%, and 44.1% higher, respectively, in mice at 3 weeks post-treatment; however, IL-17, IL-1 β and TNF- α levels were 39.8%, 58.0% and 45.6% lower, respectively, in mice at 3 weeks post-treatment than in mice at 2 days post-treatment (Fig. 7c–e).

In summary, similar to the CNS, MPTP-treated mice may develop gut inflammation in the ENS.

MPTP Damages the Intestinal Barrier in Mice

GI function and inflammation may affect the intestinal barrier. We evaluated the expression of DAO and D-LAC using ELISA to determine the degree of damage of the intestinal barrier. The expression levels of DAO and D-LAC in mice at 2 days and 3 weeks post-treatment were remarkably higher than those in the respective control mice. However, D-LAC results showed no statistically significant difference between control mice and mice at 3 weeks post-treatment. Compared with mice at 2 days post-treatment, mice at 3 weeks post-treatment showed decreases of 36.3% and 31.2% in the expression levels of DAO and D-LAC, respectively (Fig. 8a, b). Therefore, PD mice have impaired intestinal barrier performance.

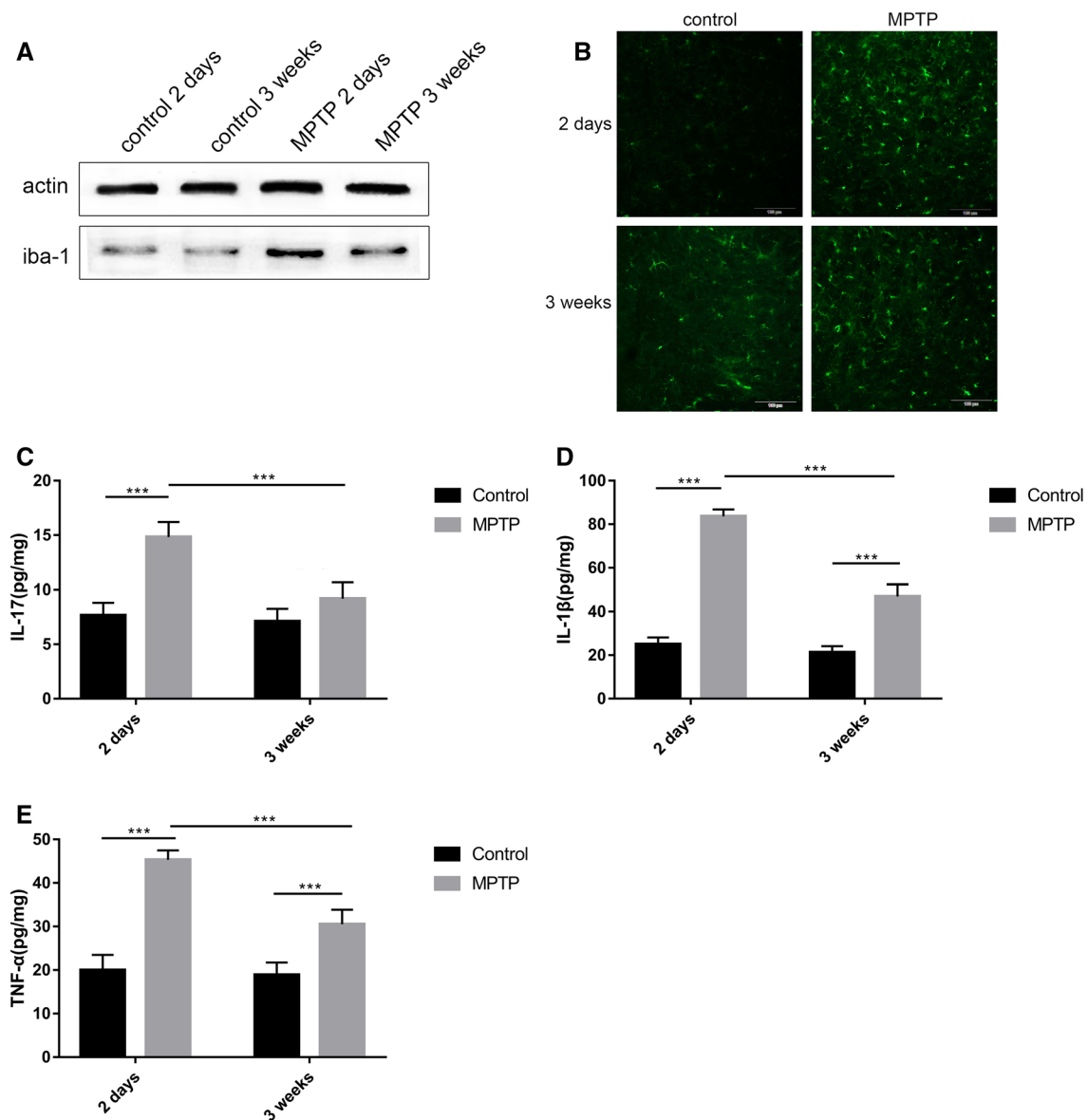


Fig. 6 MPTP causes SN inflammation in mice. **a** Representative WB of nigral Iba1 expression. **b** Representative IF staining for Iba1 in the SN. **c–e** The expression levels of nigral IL-17, IL-1β and TNF-α were measured at 2 days and 3 weeks after the last injection. **P<0.01, ***P<0.001. Error bars are SD (n=3). MPTP methyl-4-phenyl-1,2,3,6-tetrahydropyridine, SN substantia nigra, WB western blot, Iba1 ionized calcium binding adaptor molecule 1, IF immunofluorescence, SD standard deviation

MPTP Affects the Composition of Gut Microbiota in Mice

Changes in gut microbiota may also influence the pathogenesis and progression of PD. Because there was no difference between the results of the control groups at the two time points in the abovementioned studies, we merged them into the same group. Ace, Chao and Sobs were used to assess community richness, while the Simpson and Shannon indexes were used to investigate community diversity. The results of α-diversity analysis showed that there was no difference with regard to the Sobs and Simpson indexes (Fig.

S1). Both the Ace and Chao increased following 2 days of MPTP exposure compared with those in the respective control mice (Fig. 9a, b). There was a decrease in the Shannon diversity index in mice at 2 days post-treatment compared with that in control mice (Fig. 9c). Although the Ace, Chao and Shannon indexes in mice at 3 weeks post-treatment were lower than those in mice at 2 days post-treatment, these differences were not statistically significant. These results indicate a disruption of the gut microbiota.

The β-diversity analysis determines the extent of the similarity between microbial communities by measuring the degree to which membership or structure is shared between

The β-diversity analysis determines the extent of the similarity between microbial communities by measuring the degree to which membership or structure is shared between

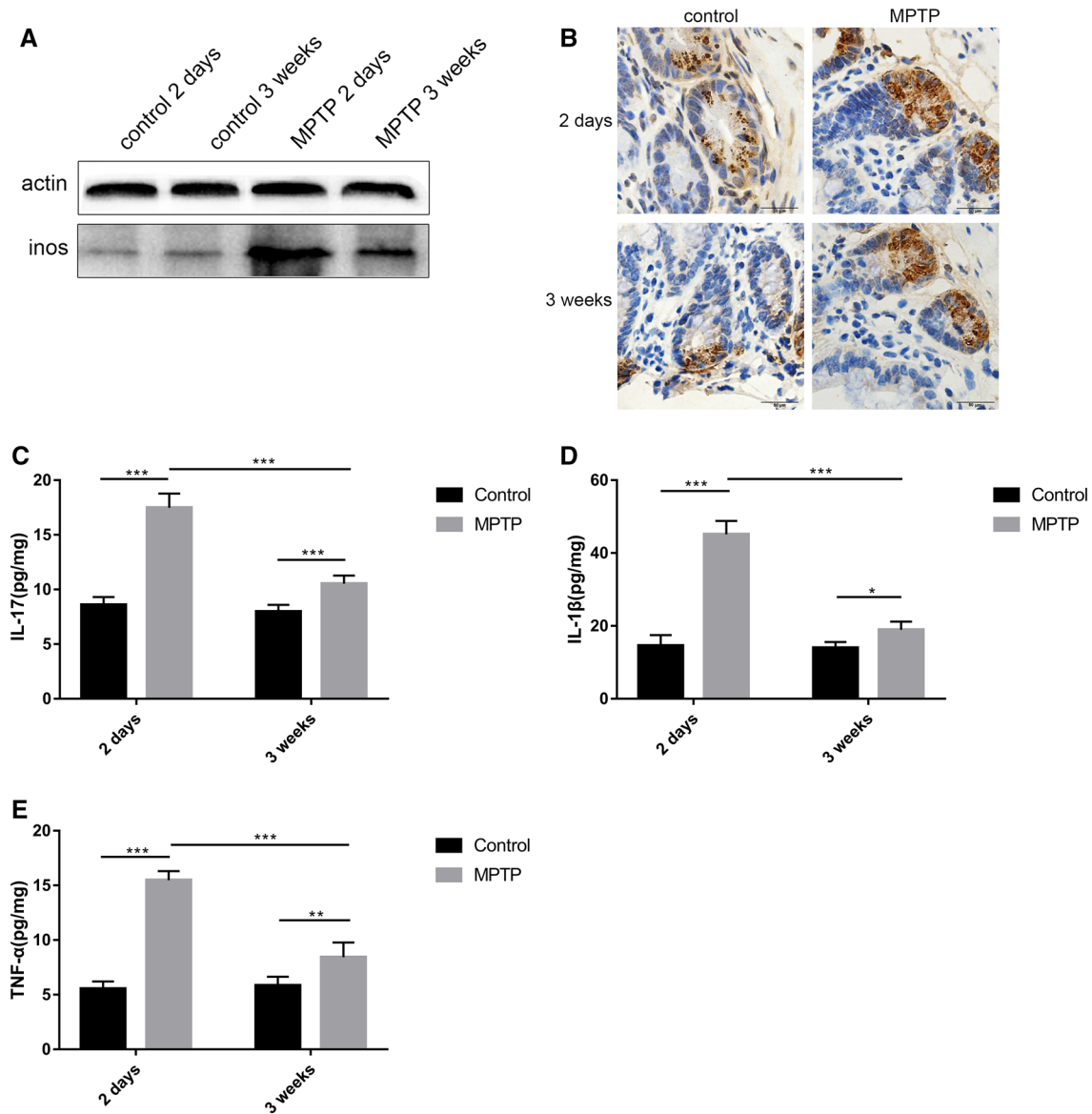


Fig. 7 MPTP causes gut inflammation in mice. **a** Representative WB of ileal iNOS expression. **b** Representative IHC staining for iNOS in the ileum. **c–e** The expression levels of ileal IL-17, IL-1 β and TNF- α were measured at 2 days and 3 weeks after the last injection.

* $P < 0.05$, ** $P < 0.01$, *** $P < 0.001$. Error bars are SD ($n = 3$). MPTP methyl-4-phenyl-1,2,3,6-tetrahydropyridine, WB western blot, iNOS inducible nitric oxide synthase, IHC immunohistochemistry, SD standard deviation

communities [31]. Based on a cluster analysis (Fig. 9d), we used PCA to analyze the overall structural changes of the gut microbiota. Although individual differences were significant, the clusters of the gut microbiota from MPTP-treated mice were clearly separated from those of control mice (Fig. 9e).

The gut bacterial community composition at the family level is shown in Fig. 9f. *Bacteroidaceae*, *Lachnospiraceae*, *Erysipelotrichaceae*, *Prevotellaceae*, *Lactobacillaceae* and *Ruminococcaceae* represented more than 80% of the gene sequences. There was no difference in *Bacteroidaceae*, *Ruminococcaceae* and other families among the groups.

The relative abundance of *Lachnospiraceae* was decreased in mice at 2 days and 3 weeks post-treatment compared with that in control mice; however, there was a statistically significant difference only between control mice and mice at 3 weeks post-treatment. The relative abundance of *Prevotellaceae* was increased in mice at 2 days post-treatment compared with that in control mice and mice at 3 weeks post-treatment; however, there was a statistically significant difference only between control mice and mice at 2 days post-treatment. Three weeks after the final MPTP injection, the relative abundance of *Erysipelotrichaceae* was significantly increased compared with that in control mice and

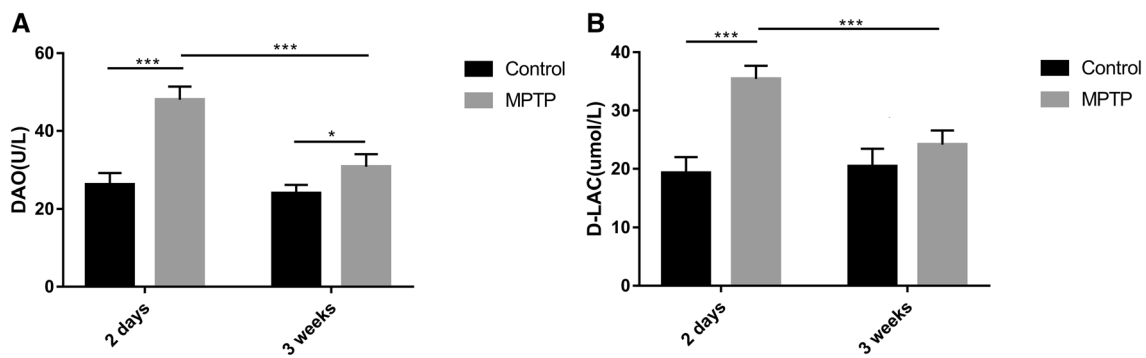


Fig. 8 MPTP damages the intestinal barrier in mice. **a** The DAO content was measured at 2 days and 3 weeks after the last injection. **b** The D-LAC content was measured at 2 days and 3 weeks after the

last injection. * $P < 0.05$, *** $P < 0.001$. Error bars are SD ($n = 3$). MPTP methyl-4-phenyl-1,2,3,6-tetrahydropyridine, DAO diamine oxidase, D-LAC D-lactic acid, SD standard deviation

mice at 2 days post-treatment. The abundance of *Lactobacillaceae* was different among the groups; however, the results were not statistically significant (Fig. 9f, g). The abundance was decreased in order *Clostridiales* in mice at 3 weeks post-treatment compared to that in control mice and was increased in order *Erysipelotrichales* in mice at 3 weeks post-treatment compared to that in control mice and mice at 2 days post-treatment (Fig. S2a). At the phylum level, decreased *Proteobacteria* was found in mice at 2 days and 3 weeks post-treatment compared to that in control mice (Fig. S2b).

These results indicate that MPTP induces gut microbial dysbiosis.

Discussion

Among PD animal models, the MPTP model is the most elaborate. In this model, different administration methods, doses, and administration times of MPTP can produce different pathological conditions. Acute MPTP administration produces the loss of DAergic neurons, and these lesions display significant levels of reversibility [32, 33]. However, chronic and low-dose administration can better reproduce the slow and progressive neurodegenerative process characteristic of PD [33]. Furthermore, this model displays a continuous neuroinflammatory reaction that is an important feature of the pathogenesis and progression of PD. Therefore, a chronic low-dose MPTP model was used to evaluate the progression of the intestinal pathology in PD, as well as whether the intestinal pathology is accompanied by alterations in the composition of the gut microbiota.

We determined that after the administration of MPTP, motor function was not significantly damaged in mice. The content of DA in the striatum at the two time points studied (2 days and 3 weeks after the last MPTP injection) was decreased by 41.5% and 13.3% respectively,

compared with that in control mice. According to previous reports, typical motor symptoms are observed in a PD animal model following approximately 50–80% depletion of striatal DA [34, 35]. Therefore, these results indicate that this model may replicate the early stage of PD; thus, this model can be used to study the intestinal pathology that occurs in the early stage of PD.

In this study, both the 1-h stool frequency and the fecal water content decreased after MPTP treatment, suggesting that the GI function is impaired, which is consistent with the presentation of PD patients. Intraperitoneal injection of an acute dose of MPTP results in a transient increase in colon motility after 2–3 days of treatment [10] and delayed transit and constipation at 7 days after lesion induction [11]. The diverse results observed may be a result of the different administration times of MPTP; however, it seems that the chronic model can simulate the GI dysfunction of PD patients better than the acute model. After 3 weeks of MPTP removal, the GI dysfunction recovered slightly; however, the GIT continued to display persistent damage. To date, no report has addressed the effect of chronic low-dose MPTP lesions on GI dysfunction in mice.

We used the ileum as a representation of the GIT to study its pathology. Following MPTP administration, the DA content of the ileum was decreased, and the TH expression in the ileum was increased, which is inconsistent with previous reports using MPTP in mice [12, 27]. A reasonable explanation may be that when the secretion of DA in the ileum is reduced, there is a compensatory increase in the synthesis of TH. However, the levels of TH and DA at 3 weeks post-treatment show that the damage lasts 3 weeks and that the levels do not return to those of the control animals. Interestingly, both the DA content and the TH expression in the SN were significantly decreased after MPTP treatment (Figs. 3a, 4a, b), and the TH expression was further decreased at 3 weeks post-treatment (Fig. 4a, b). The differential results in the SN

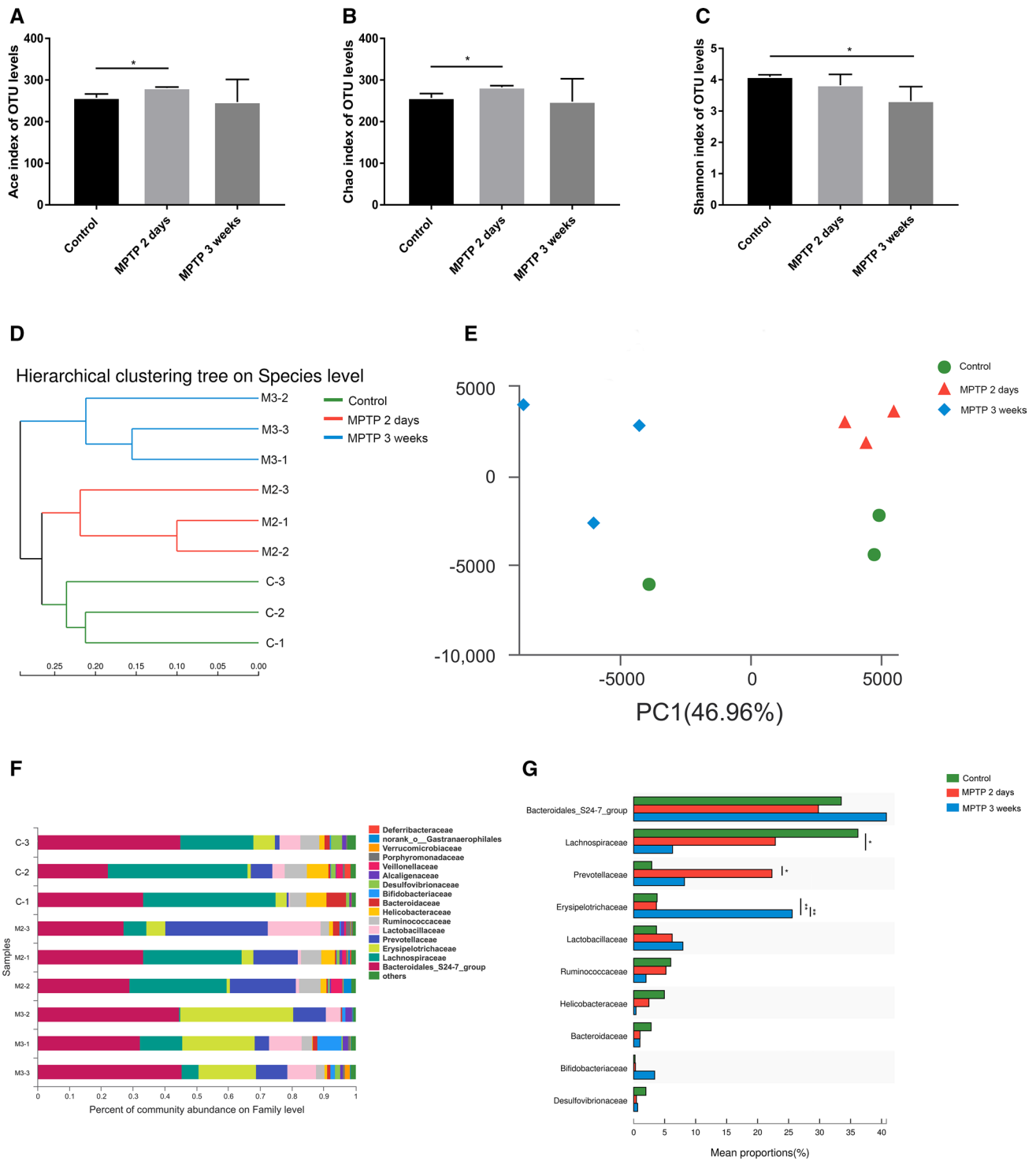


Fig. 9 MPTP affects the composition of gut microbiota in mice. **a–c** Representative indexes of α -diversity, including Ace, Chao and Shannon. **d** Clustering analysis of gut microbiota. **e** PCA score plot of gut microbiota. **f** Relative abundance of gut microbiota at the family level

among different groups. **g** Comparisons of the relative abundance at the family level. * $P < 0.05$, ** $P < 0.01$. Error bars are SD ($n = 3$). MPTP methyl-4-phenyl-1,2,3,6-tetrahydropyridine, PCA principal component analysis, SD standard deviation

and ileum indicate that the SN may be more sensitive to MPTP than the ileum.

In PD patients and PD models, α -syn aggregates in the brain and gut. However, our research did not indicate the accumulation of α -syn, but the expression was decreased, which confirms previous findings in the acute phase [36]. These different results indicate that further studies are necessary to better understand the pathogenesis of α -syn.

In this model, MPTP caused the significant pathological damage to the midbrain and ileum. Pearson correlations were applied to associate damage in the midbrain and damage in the ileum. There was no correlation between the DA content in the striatum and the DA content in the ileum (data not shown). Similarly, TH expression in the SN had no correlation with TH expression in the ileum (data not shown) and α -syn expression in the SN also had no correlation with α -syn expression in the ileum (data not shown). However, we suggest that more samples are needed to verify these results. For example, we can select samples from additional time points after treatment to detect alterations.

Inflammation has been shown to play a crucial part in PD pathogenesis. An appropriate inflammatory response can promote the repair of injury, while a sustained excessive inflammatory reaction results in further damage. We and other researchers have shown that the factors related to inflammation were strongly increased in both the SN and the ileum after MPTP administration [12, 37]. We hypothesize that inflammation may affect intestinal permeability, which in turn causes damage to the intestinal barrier. Three weeks after MPTP was removed, the factors related to inflammation and the damaged intestinal barrier did not recover to the control level, indicating persistent inflammation.

At present, it is recognized the gut microbiota may play an important role in progression of PD. But there are a few reports on gut microbial dysbiosis in PD patients and animal models, and the results are diversity. Studies have indicated that there are no statistically significant differences in common α -diversity indexes between controls and PD patients [6, 38]. However, changes in α -diversity have been reported between control and MPTP-treated mice [37, 39], which was shown in our study. Given that gut microbial dysbiosis occurs in PD patients [38, 40], we also proved discrepancies in the composition of the gut microbiota in PD mice. Similar to other studies [6, 37–39], the β -diversity analysis results were different between controls and patients or PD mice. We determined that the abundance of *Prevotellaceae* was increased after MPTP administration, which contrasts with findings in PD patients [6, 17, 41]. *Lachnospiraceae*, which has been associated with the maintenance of gut health [42, 43], was decreased in our PD mice. *Erysipelotrichaceae*, a bacterial family assigned to the phylum of *Firmicutes*, was increased in our PD mice. The abundance of *Erysipelotrichaceae* was increased in inflammation-related

GIT diseases, such as colorectal cancer and inflammatory bowel disease [44]. However, there have been no reports of changes in the *Lachnospiraceae* and *Erysipelotrichaceae* composition in PD. The abundance of *Firmicutes* did not differ between control and MPTP-treated mice (Fig. S2), which contrasted with several studies [37, 45]. The abundance of *Akkermansia* was increased in our PD mice, which is consistent with findings in PD patients [17]; however, the difference was not significant (Fig. S3). There is no research regarding *Clostridiales* and *Erysipelotrichales* in PD at present; however, it has been reported that *Clostridiales* is related to irritable bowel syndrome (IBS) [46]. *Proteobacteria* has been showed to be connected to GI inflammation, and it was significantly more abundant in the mucosa of PD patients [45, 47]. We infer that these diverse results might be in part due to the PD stage progression and the small number of samples studied; thus, further studies are required.

In conclusion, the present study demonstrates that PD model animals constructed with chronic and low-dose MPTP develop persistent pathological lesions and gut microbial dysbiosis. Changes in the composition of the gut microbiota might be involved in the pathogenesis of PD. Because there are no effective therapies for PD, we will focus on whether it is possible to postpone the progression of PD by improving gut microbial dysbiosis.

Acknowledgements The present study was supported by the Chongqing Yuzhong Nature Science Foundation of China (Grant No. 20160121).

Compliance with Ethical Standards

Conflict of interest The authors declare that they have no conflict of interest.

References

- Dickson DW (2018) Neuropathology of Parkinson disease. *Parkinsonism Relat Disord* 46(Suppl 1):S30–S33. <https://doi.org/10.1016/j.parkreldis.2017.07.033>
- Kalia LV, Lang AE (2015) Parkinson's disease. *Lancet* 386(9996):896–912. [https://doi.org/10.1016/s0140-6736\(14\)61393-3](https://doi.org/10.1016/s0140-6736(14)61393-3)
- Hussl A, Seppi K, Poewe W (2013) Nonmotor symptoms in Parkinson's disease. *Expert Rev Neurother* 13(6):581–583. <https://doi.org/10.1586/ern.13.53>
- Fasano A, Visanji NP, Li LWC, Lang AE, Pfeiffer RF (2015) Gastrointestinal dysfunction in Parkinson's disease. *Lancet Neurol* 14(6):625–639. [https://doi.org/10.1016/s1474-4422\(15\)00007-1](https://doi.org/10.1016/s1474-4422(15)00007-1)
- Clairembault T, Leclair-Visonneau L, Coron E, Bourreille A, Le Dily S, Vavasseur F, Heymann MF, Neunlist M, Derkinderen P (2015) Structural alterations of the intestinal epithelial barrier in Parkinson's disease. *Acta Neuropathol Commun* 3:12. <https://doi.org/10.1186/s40478-015-0196-0>
- Scheperjans F, Aho V, Pereira PA, Koskinen K, Paulin L, Pekkonen E, Haapaniemi E, Kaakkola S, Eerola-Rautio J, Pohja M, Kinnunen E, Murros K, Auvinen P (2015) Gut microbiota are

- related to Parkinson's disease and clinical phenotype. *Mov Disord* 30(3):350–358. <https://doi.org/10.1002/mds.26069>
7. Braak H, Rub U, Gai WP, Del Tredici K (2003) Idiopathic Parkinson's disease: possible routes by which vulnerable neuronal types may be subject to neuroinvasion by an unknown pathogen. *J Neural Transm* 110(5):517–536. <https://doi.org/10.1007/s00702-002-0808-2>
 8. Braak H, de Vos RA, Bohl J, Del Tredici K (2006) Gastric alpha-synuclein immunoreactive inclusions in Meissner's and Auerbach's plexuses in cases staged for Parkinson's disease-related brain pathology. *Neurosci Lett* 396(1):67–72. <https://doi.org/10.1016/j.neulet.2005.11.012>
 9. Phillips RJ, Walter GC, Wilder SL, Baronowsky EA, Powley TL (2008) Alpha-synuclein-immunopositive myenteric neurons and vagal preganglionic terminals: autonomic pathway implicated in Parkinson's disease? *Neuroscience* 153(3):733–750. <https://doi.org/10.1016/j.neuroscience.2008.02.074>
 10. Anderson G, Noorian AR, Taylor G, Anitha M, Bernhard D, Srinivasan S, Greene JG (2007) Loss of enteric dopaminergic neurons and associated changes in colon motility in an MPTP mouse model of Parkinson's disease. *Exp Neurol* 207(1):4–12. <https://doi.org/10.1016/j.expneurol.2007.05.010>
 11. Natale G, Kastsiushenka O, Fulceri F, Ruggieri S, Paparelli A, Fornai F (2010) MPTP-induced parkinsonism extends to a subclass of TH-positive neurons in the gut. *Brain Res* 1355:195–206. <https://doi.org/10.1016/j.brainres.2010.07.076>
 12. Poirier AA, Cote M, Bourque M, Morissette M, Di Paolo T, Soulet D (2016) Neuroprotective and immunomodulatory effects of raloxifene in the myenteric plexus of a mouse model of Parkinson's disease. *Neurobiol Aging* 48:61–71. <https://doi.org/10.1016/j.neurobiolaging.2016.08.004>
 13. Martin CR, Osadchiv V, Kalani A, Mayer EA (2018) The brain-gut-microbiome axis. *Cell Mol Gastroenterol Hepatol*. <https://doi.org/10.1016/j.jcmgh.2018.04.003>
 14. Foster JA, McVey Neufeld KA (2013) Gut-brain axis: how the microbiome influences anxiety and depression. *Trends Neurosci* 36(5):305–312. <https://doi.org/10.1016/j.tins.2013.01.005>
 15. Vuong HE, Hsiao EY (2017) Emerging roles for the gut microbiome in autism spectrum disorder. *Biol Psychiatry* 81(5):411–423. <https://doi.org/10.1016/j.biopsych.2016.08.024>
 16. Mancuso C, Santangelo R (2018) Alzheimer's disease and gut microbiota modifications: the long way between preclinical studies and clinical evidence. *Pharmacol Res* 129:329–336. <https://doi.org/10.1016/j.phrs.2017.12.009>
 17. Unger MM, Spiegel J, Dillmann KU, Grundmann D, Philippeit H, Burmann J, Fassbender K, Schwiertz A, Schafer KH (2016) Short chain fatty acids and gut microbiota differ between patients with Parkinson's disease and age-matched controls. *Parkinsonism Relat Disord* 32:66–72. <https://doi.org/10.1016/j.parkreldis.2016.08.019>
 18. Hirsch EC, Vyas S, Hunot S (2012) Neuroinflammation in Parkinson's disease. *Parkinsonism Relat Disord* 18:S210–S212. [https://doi.org/10.1016/s1353-8020\(11\)70065-7](https://doi.org/10.1016/s1353-8020(11)70065-7)
 19. Sawada M, Imamura K, Nagatsu T (2006) Role of cytokines in inflammatory process in Parkinson's disease. *J Neural Transm Suppl* 70:373–381
 20. Ito D, Imai Y, Ohsawa K, Nakajima K, Fukuuchi Y, Kohsaka S (1998) Microglia-specific localisation of a novel calcium binding protein, Iba1. *Brain Res Mol Brain Res* 57(1):1–9
 21. Imai Y, Kohsaka S (2002) Intracellular signaling in M-CSF-induced microglia activation: role of Iba1. *Glia* 40(2):164–174. <https://doi.org/10.1002/glia.10149>
 22. Hisahara S, Shimohama S (2010) Toxin-induced and genetic animal models of Parkinson's disease. *Parkinson's Dis* 2011:951709. <https://doi.org/10.4061/2011/951709>
 23. Nicotra A, Parvez SH (2000) Cell death induced by MPTP, a substrate for monoamine oxidase B. *Toxicology* 153(1–3):157–166
 24. Perry TL, Yong VW, Jones K, Wall RA, Clavier RM, Foulks JG, Wright JM (1985) Effects of N-methyl-4-phenyl-1,2,3,6-tetrahydropyridine and its metabolite, N-methyl-4-phenylpyridinium ion, on dopaminergic nigrostriatal neurons in the mouse. *Neurosci Lett* 58(3):321–326
 25. Cote M, Drouin-Ouellet J, Cicchetti F, Soulet D (2011) The critical role of the MyD88-dependent pathway in non-CNS MPTP-mediated toxicity. *Brain Behav Immun* 25(6):1143–1152. <https://doi.org/10.1016/j.bbi.2011.02.017>
 26. Xiao-Feng L, Wen-Ting Z, Yuan-Yuan X, Chong-Fa L, Lu Z, Jin-Jun R, Wen-Ya W (2016) Protective role of 6-hydroxy-1-H-indazole in an MPTP-induced mouse model of Parkinson's disease. *Eur J Pharmacol* 791:348–354. <https://doi.org/10.1016/j.ejphar.2016.08.011>
 27. Ellett LJ, Hung LW, Munckton R, Sherratt NA, Culvenor J, Grubman A, Furness JB, White AR, Finkelstein DI, Barnham KJ, Lawson VA (2016) Restoration of intestinal function in an MPTP model of Parkinson's Disease. *Sci Rep* 6:30269. <https://doi.org/10.1038/srep30269>
 28. Lawson VA, Furness JB, Klemm HM, Pontell L, Chan E, Hill AF, Chiochetti R (2010) The brain to gut pathway: a possible route of prion transmission. *Gut* 59(12):1643–1651. <https://doi.org/10.1136/gut.2010.222620>
 29. Xu N, Tan G, Wang H, Gai X (2016) Effect of biochar additions to soil on nitrogen leaching, microbial biomass and bacterial community structure. *Eur J Soil Biol* 74:1–8. <https://doi.org/10.1016/j.ejsobi.2016.02.004>
 30. Cote M, Bourque M, Poirier AA, Aube B, Morissette M, Di Paolo T, Soulet D (2015) GPER1-mediated immunomodulation and neuroprotection in the myenteric plexus of a mouse model of Parkinson's disease. *Neurobiol Dis* 82:99–113. <https://doi.org/10.1016/j.nbd.2015.05.017>
 31. Ling Z, Jin C, Xie T, Cheng Y, Li L, Wu N (2016) Alterations in the fecal microbiota of patients with HIV-1 infection: an observational study in a Chinese population. *Sci Rep* 6:30673. <https://doi.org/10.1038/srep30673>
 32. Klingelhofer L, Reichmann H (2015) Pathogenesis of Parkinson disease: the gut-brain axis and environmental factors. *Nat Rev Neurol* 11(11):625–636. <https://doi.org/10.1038/nrneuro.2015.197>
 33. Munoz-Manchado AB, Villadiego J, Romo-Madero S, Suarez-Luna N, Bermejo-Navas A, Rodriguez-Gomez JA, Garrido-Gil P, Labandeira-Garcia JL, Echevarria M, Lopez-Barneo J, Toledo-Aral JJ (2016) Chronic and progressive Parkinson's disease MPTP model in adult and aged mice. *J Neurochem* 136(2):373–387. <https://doi.org/10.1111/jnc.13409>
 34. Duty S, Jenner P (2011) Animal models of Parkinson's disease: a source of novel treatments and clues to the cause of the disease. *Br J Pharmacol* 164(4):1357–1391. <https://doi.org/10.1111/j.1476-5381.2011.01426.x>
 35. Bezdard E, Dovero S, Prunier C, Ravenscroft P, Chalou S, Guillo-teau D, Crossman AR, Bioulac B, Brotchie JM, Gross CE (2001) Relationship between the appearance of symptoms and the level of nigrostriatal degeneration in a progressive 1-methyl-4-phenyl-1,2,3,6-tetrahydropyridine-lesioned macaque model of Parkinson's disease. *J Neurosci* 21(17):6853–6861
 36. Drolet RE, Cannon JR, Montero L, Greenamyre JT (2009) Chronic rotenone exposure reproduces Parkinson's disease gastrointestinal neuropathology. *Neurobiol Dis* 36(1):96–102. <https://doi.org/10.1016/j.nbd.2009.06.017>
 37. Sun MF, Zhu YL, Zhou ZL, Jia XB, Xu YD, Yang Q, Cui C, Shen YQ (2018) Neuroprotective effects of fecal microbiota transplantation on MPTP-induced Parkinson's disease mice: gut microbiota, glial reaction and TLR4/TNF-alpha signaling pathway. *Brain Behav Immun* 70:48–60. <https://doi.org/10.1016/j.bbi.2018.02.005>

38. Li W, Wu X, Hu X, Wang T, Liang S, Duan Y, Jin F, Qin B (2017) Structural changes of gut microbiota in Parkinson's disease and its correlation with clinical features. *Sci China Life Sci* 60(11):1223–1233. <https://doi.org/10.1007/s11427-016-9001-4>
39. Yang X, Qian Y, Xu S, Song Y, Xiao Q (2017) Longitudinal analysis of fecal microbiome and pathologic processes in a rotenone induced mice model of Parkinson's disease. *Front Aging Neurosci* 9:441. <https://doi.org/10.3389/fnagi.2017.00441>
40. Hill-Burns EM, Debelius JW, Morton JT, Wissemann WT, Lewis MR, Wallen ZD, Peddada SD, Factor SA, Molho E, Zabetian CP, Knight R, Payami H (2017) Parkinson's disease and Parkinson's disease medications have distinct signatures of the gut microbiome. *Mov Disord* 32(5):739–749. <https://doi.org/10.1002/mds.26942>
41. Vizcarra JA, Wilson-Perez HE, Espay AJ (2015) The power in numbers: gut microbiota in Parkinson's disease. *Mov Disord* 30(3):296–298. <https://doi.org/10.1002/mds.26116>
42. Antharam VC, Li EC, Ishmael A, Sharma A, Mai V, Rand KH, Wang GP (2013) Intestinal dysbiosis and depletion of butyrogenic bacteria in *Clostridium difficile* infection and nosocomial diarrhea. *J Clin Microbiol* 51(9):2884–2892. <https://doi.org/10.1128/jcm.00845-13>
43. Biddle A, Stewart L, Blanchard J, Leschine S (2013) Untangling the genetic basis of fibrolytic specialization by Lachnospiraceae and Ruminococcaceae in diverse gut communities. *Diversity* 5(3):627–640. <https://doi.org/10.3390/d5030627>
44. Kaakoush NO (2015) Insights into the role of Erysipelotrichaceae in the human host. *Front Cell Infect Microbiol* 5:84. <https://doi.org/10.3389/fcimb.2015.00084>
45. Keshavarzian A, Green SJ, Engen PA, Voigt RM, Naqib A, Forsyth CB, Mutlu E, Shannon KM (2015) Colonic bacterial composition in Parkinson's disease. *Mov Disord* 30(10):1351–1360. <https://doi.org/10.1002/mds.26307>
46. Gargari G, Taverniti V, Gardana C, Cremon C, Canducci F, Pagano I, Barbaro MR, Bellacosa L, Castellazzi AM, Valsecchi C, Tagliacarne SC, Bellini M, Bertani L, Gambaccini D, Marchi S, Cicala M, Germana B, Dal Pont E, Vecchi M, Ogliari C, Fiore W, Stanghellini V, Barbara G, Guglielmetti S (2018) Fecal Clostridiales distribution and short-chain fatty acids reflect bowel habits in irritable bowel syndrome. *Environ Microbiol*. <https://doi.org/10.1111/1462-2920.14271>
47. Carvalho FA, Koren O, Goodrich JK, Johansson ME, Nalbantoglu I, Aitken JD, Su Y, Chassaing B, Walters WA, Gonzalez A, Clemente JC, Cullender TC, Barnich N, Darfeuille-Michaud A, Vijay-Kumar M, Knight R, Ley RE, Gewirtz AT (2012) Transient inability to manage proteobacteria promotes chronic gut inflammation in TLR5-deficient mice. *Cell Host Microbe* 12(2):139–152. <https://doi.org/10.1016/j.chom.2012.07.004>